

# **TERRAIN FEATURE EXTRACTION FROM VARIABLE RESOLUTION DIGITAL ELEVATION MODELS**

Keith C. Clarke and Reginald Archer  
Department of Geography  
University of California, Santa Barbara  
Santa Barbara  
CA 93106-4060 USA  
{kclarke, archer}@geog.ucsb.edu

## **ABSTRACT**

In this paper, we address the impact of changing spatial resolution and terrain type on the geometry of stream systems and drainage basins as extracted from digital elevation models (DEMs) using automated terrain feature extraction methods. Five different resolutions for each of three terrain types were analyzed to derive stream vectors for comparison using several standard hydrological metrics. First, we demonstrate that the generation of drainage and watershed features using ArcGIS's Arc Hydro tools reveals major structural geometric differences in specific terrain parameters when tested across terrain types. Unexpectedly, mixed terrain with only moderate relief shows more variance than flat or hilly terrain, though flat terrain has some very distinct scale behaviors. Second, as resolution in terms of cell size gets smaller, there is a measurable increase in many terrain parameters, sufficient to definitively state that there are significant scale dependencies in the parameters. Finally, we indicate that LiDAR data demonstrates this increase in variance effect. The results of this analysis may lead to new algorithms and approaches that use LiDAR to achieve higher levels of accuracy in terrain feature extraction from DEMs.

## **INTRODUCTION**

The upper terrain surface of the landscape can be divided into a set of non-overlapping, exhaustive polygonal regions that characterize landscape features with common descriptive terms, the boundaries of which are often called the surface network. These features include lakes, drainage lines, ridges, valleys, hillslopes, saddles, and depressions. In future geographic information systems these and other features, rather than map tiles, will be the basis for storing attributes and searching data, in the so-called object model for GIS. The features can be extracted automatically by processing digital elevation models (DEMs) using both off-the-shelf routines and custom algorithms. Identification of these features for automated labeling is an important step not only for further analysis, but also for building a consistent ontology of map features and for subsequent tasks such as map search and feature annotation. Natural terrain features have been extracted by computing downslope flow accumulation from a DEM, and thresholding these values to extract drainage and ridge vectors (Wilson and Gallant, 2000).

A significant improvement in DEM accuracy and resolution has resulted from the widespread use of LiDAR in mapping terrain (NRC, 2007). Increased precision and resolution has driven a need to characterize these terrain features more precisely, so that

they can also be conflated with other features in the map ontology, such as roads and cultural features. In this study, we examined the impact that using higher resolution DEMs has on the feature extraction process. We used one extraction procedure, but tested its efficacy across different spatial resolutions and with three types of DEM: flat, rolling topography, and mountainous, from North Carolina, USA.

The innovative aspect of this approach is that while data fusion in the geospatial sciences has often been seen as a major problem for future systems development, few practical demonstrations using existing data and suites of methods exist, and the impacts of merging different measurement instruments and resolutions remain largely unexplored. Carrara et al. (2008) designed a multi-source fusion system for environmental data using ordered weighted averaging, noting the problems of missing data and merging data of different quality, issues covered for medium-resolution imagery by Roy et al. (2008). Duckham and Worboys (2005) presented a method for information fusion using an automated algorithm that infers the schema-level structure from instance-level data, using the example of land cover. Ling et al. (2008) looked specifically at resolution sensitivity during fusion, for remote sensing data of Camp Lejeune, NC. They used a ratio of resolutions, and showed that image quality decreases as the ratio moves from 1:10 to 1:30, indicating that there is a limited spatial range at which fusion is effective. Nikolakopoulos (2008) quantitatively compared nine different image fusion methods, but did not consider higher resolution data such as LiDAR or fusion across themes. The value of LiDAR as being of significant benefit in detailing topography has not escaped the imagery fusion research. Tong and Deng (2008) have looked at the cartographic implications for map fusion, with an emphasis on error detection. Chen et al. (2006) have looked at conflating vector data with imagery for roads, while Elaksher (2008) has looked at fusing LiDAR-based DEMs and hyperspectral imagery in the littoral zone. Pu and Vosselman (2009) extended the fusion approach to terrestrial LiDAR scans of urban landscapes. Liu has recently examined the challenges of LiDAR-based DEM generation methods.

There have been recent advances in the formalization of the terrain surface and its skeleton (Deng, 2007). Critical metrics for classifying terrain objects are elevation, surface shape, topographic position, topographic context, spatial form, and landscape object. These can be used to create five categories of prototypical objects. Chevriaux et al. (2005) have shown that many of these are the result of simple topological relations on the surface. The implication is that detailed terrain can be unraveled into sets of terrain metrics, and then recombined into morphometric and feature classes using clustering and clumping methods. We seek to answer the question of which metrics are associated with which features by conducting empirical experiments across scales.

LiDAR is a relatively new and transformational data source for terrain mapping, capable of extraordinary accuracy. It adds the point cloud and the upper and lower terrain surfaces to the traditional forms for storing digital terrain, i.e. regular grids, points, triangulated irregular networks, and contours. Kraus and Pfeifer (1998) demonstrated that LiDAR DEM generation, even in forests, exceeds the accuracy of that for bare ground using the best alternative, photogrammetry. Accuracy can be 15 cm root-mean-squared error vertically, and 20 cm horizontally (BC-CARMS, 2006). In addition, and unlike



**Figure 1** Original Color DOQQ for the three study areas. 1) Hilly area in Caldwell, NC; 2) Mixed relief in McDowell and Burke Counties, and 3) Flat (urban) terrain in Durham County, NC.

many other mapping methods, LiDAR penetrates most surface cover, such as vegetation, and gives multiple elevation returns. Typically, the first and last laser pulse returns show the top and bottom of the vegetation canopy. Return intensity and the return heights can be used in several ways to create heights of the surface. These LiDAR returns, the full LiDAR point cloud, plus existing ancillary data such as imagery, can enhance the automatic extraction of terrain information. Accurate mapping of bare earth terrain is valuable for many purposes e.g. flood management, land subsidence, land disturbance, and erosion/deposition assessment (NRC, 2007).

In this paper, we address the impact of changing spatial resolution and terrain type on the geometry of the terrain surface, specifically the drainage channels and watershed outline, as generated by Arc Hydro tools within the ESRI ArcGIS software. This tool was selected because we wanted a common off-the-shelf approach that is frequently used in real-world applications. We hypothesize that drainage feature extraction methods will show sensitivity, measured by variance from a control solution, that increases as relief decreases, and that also increases as resolution becomes finer. Furthermore, we hypothesize that LiDAR resolutions are close to, or exceed, the level when extraction error becomes dominant in delineating the surface features. Should this be correct, new or vastly improved methods for terrain feature extraction will be necessary when dealing with LiDAR-derived terrain data.

Past studies have shown that terrain analysis methods based on different DEM sources, grid resolutions and flow routing methods can have a large impact on the magnitude and spatial pattern of computed topographic attributes (Wilson et al, 2000). In addition, sensitivity analysis of computed terrain attributes showed that higher resolution DEMs, between 2m and 10m cell spacing, performed better than lower 30m and 90m resolutions (Clarke and Lee, 2007). The main limitations of these studies are that they did not consider LiDAR as a data source and that many of the hydro-processing software tools have yet to be tested with very high resolution data. Under normal conditions, when higher resolution data are available it is automatically assumed that superior results are achieved. In this study, we challenge this simple assumption.

## **DATA**

We examined the ability of GIS software to identify and characterize topographic surface features (stream drainage channels and ridge lines) as a function of DEM resolution and terrain type for three selected areas in North Carolina, USA. To accomplish the characterization task, we used Arc Hydro within ESRI's ArcGIS software (Maidment, 2002), because the drainage feature extraction procedures are well documented and are believed to be robust. The Arc Hydro routines follow a typical extraction procedure: pit filling, computation of the direction of maximum downslope movement, flow accumulation, thresholding and lastly vectorization. The sources of elevation data include: National Elevation Data (NED) datasets at 3m, 10m and 30m resolutions; Shuttle Radar Topography Mission (SRTM) data at 30m; and LiDAR data from the North Carolina Department of Transportation (NCDOT) at a vertical resolution of one foot and a horizontal resolution of 6.096m (20 feet) with a root-mean squared vertical error of 20cm. The 3m NED data are the result of updating the 10m NED by adding data from the LiDAR point cloud, and so represent fused data.

These data were selected because they were available in the public domain through the USGS National Map seamless server. All NED data are distributed in geographic coordinates in units of decimal degrees, referenced to the North American Datum of 1983 (NAD 83). All elevation values are provided in units of meters, on the North American Vertical Datum of 1988 (NAVD 88). Integerized units of vertical elevation means that vertical resolution is 0.033, 0.1, 0.164 (m) and 0.05 (ft.), and 0.33 of the horizontal resolution, implying differential surface approximations at the different resolutions. NED data are available nationally at resolutions of 1 arc-second (approximately 30 meters) and 1/3 arc-second (approximately 10 meters), and in limited areas at 1/9 arc-second (approximately 3 meters). NED 1/9 arc-second data (3 meter resolution at this latitude) is processed and assembled the same as the NED 1 and 1/3 arc second, but the source data is using mostly LIDAR elevation data and so far there is not extensive coverage outside of North Carolina. The DEMs can be downloaded free from the U.S. Geological Survey (USGS) portals <<http://nationalmap.gov>> or <<http://seamless.usgs.gov>>. Other data come from a global DEM from the Shuttle Radar Topographic Mapping mission (SRTM), computed using C-band RADAR interferometry (Rabus et al., 2003). SRTM 30m resolution data was also downloaded from the USGS seamless server. These data are known to have been post-processed to remove the effects of RADAR backscatter, especially within water bodies. NCDOT LiDAR data was released in May 2007, all data were collected using airborne LiDAR in April 2007 and is in North Carolina State Plane feet registered to NAD83. Spatial resolution is 6.096m (20 ft.), as interpolated from the irregular point cloud data. The data was chosen for regions with varying relief for analysis across terrain types. Three different terrain relief types were selected: Hilly (high relief), Mixed (medium relief) and Flat (low relief) terrain. The study sites are located in portions of Caldwell (hilly), Burke & McDowell (mixed) and Durham (flat), counties in North Carolina. Figure 1 shows the varying relief in the three areas. The flat terrain included urban land uses.

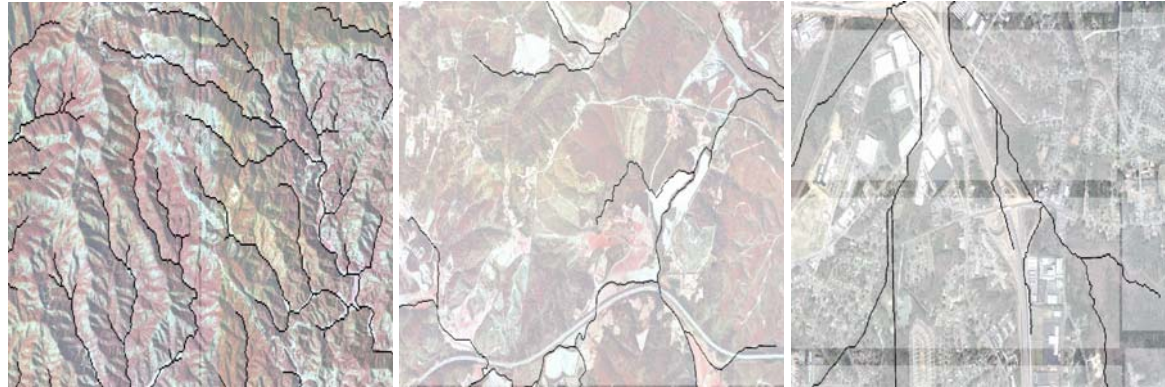


**Figure 2:** Examples of DEM derived stream networks for each terrain type.  
 Left: Hilly: 30m SRTM. Center: Mixed: 10m NED. Right: Flat: LiDAR 6.1m

To compute each set of terrain parameters, data was extracted at each resolution, i.e. 30m (NED), 30m (SRTM), 10m, and 6.1m and 3m for the LiDAR DEM. These five different resolutions for each terrain type were analyzed to derive stream delineations for comparison. ArcGIS 9.3 and Arc Hydro were used to extract stream channel networks to be characterized in the final analysis. Several hydrology tools are part of the basic Spatial Analyst extension of ArcGIS, and Arc Hydro incorporates many more tools for hydro-processing beyond those employed.

## METHODS

Once the DEMs were uploaded into ArcGIS, the first step in the stream delineation is to fill any enclosed depressions or sinks found in the DEMs using the Arc Hydro default threshold values: “Fill All” to build a new DEM with all the depressions filled. The next steps include creating a flow direction grid based on the new DEM, and then extracting a flow accumulation grid based on the flow direction grid. Flow direction is the direction of the vector of maximum downslope gradient. Arc Hydro computes this using an eight (8) direction pour point model in a 3×3 grid. It is assumed that the water has only eight possible directions in each grid cell. The eight directions are assigned the numbers 1,2,4,8,16,32,64 and 128, in the order of east, southeast, south, southwest, west, northwest, north and northeast (Maidment, 2002). The third pre-processing step creates a flow accumulation grid from the flow direction grid. We used the flow accumulation grid to determine the stream network for each resolution in each terrain type. Figure 2 shows examples of the stream networks identified within each terrain type for a subset of the data. With five DEM resolutions and three terrain types, a total of 15 applications of automated drainage channel extraction were performed. Since there was no independent source of higher authority with which to compare the extracted streams, we used the 1m Digital Orthophoto Quarter Quadrangle, known to be of high geometric fidelity, as ground truth. At very high resolutions, stream existence is a fuzzy concept, since channels are near the data resolution, so only visual comparisons to the best available data were made.

Statistical cross-comparisons by resolutions and types were possible by computing derived terrain parameters. We computed the following statistics: (1) the Strahler stream order and its aggregate descriptors (streams by order, and branching ratio); (2) total flow



path lengths; and (3) total downslope flow accumulation means and maxima. We also examined detailed focal studies, to show where there were major discrepancies among the data sets.

## RESULTS

First among the computed statistics was the division by Strahler stream order (Strahler, 1957). This simple measure takes each stream segment, and moving downstream, numbers the segments by their degree of convergence. At the uppermost limit, all segments are labeled “1”, and whenever two streams of the same order meet at a confluence point, the downstream segment increases in order by one. This allows the computation of the bifurcation or branching ratio. For each order  $i$  in a hierarchy, the  $i$ -th bifurcation ratio is  $(n_{i-1})/(n_i)$  where  $n_i$  denotes the number of nodes with order  $i$ .

Figure 3 shows the number of segments extracted by type of DEM and classified by Strahler order. The ordering of the number of segments and their structure by Strahler order is what would be expected, a function of resolution. The greatest differences by resolution are at the lower stream orders, where for the flat terrain the 3m DEM generated 10990 segments as opposed to 1011 from the 30m NED and 1124 from the 30m SRTM DEM. This maximum at 3m corresponded to 22731 streams segments for the mixed terrain, and 13118 for the hilly terrain. Corresponding minima for the STRM DEM at 30m and at Strahler level 4 were 46 for flat, 60 for mixed, and 0 for hilly. Clearly, as the stream order increases there is less difference among the different resolutions, again as would be expected.

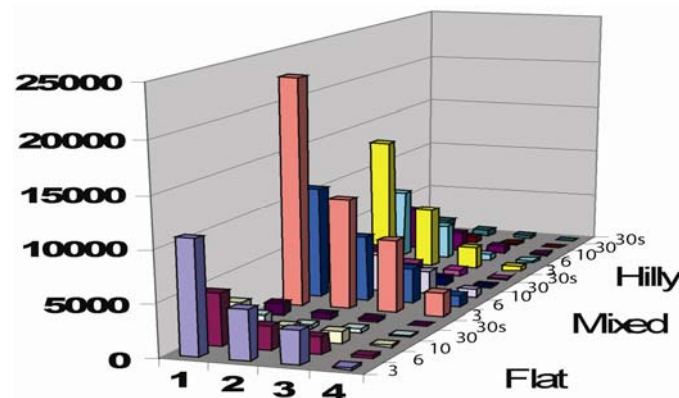


**Figure 3:** Number of Stream Segments by Strahler Order, Resolution and Terrain Type

Figure 3 also shows the mean Strahler order frequency by terrain type, showing that the differences in the depth of the stream hierarchy diminish as the resolution becomes coarser. It is clear that while the ordering by resolution is fairly constant across the three terrains, the raw numbers of stream segments vary by a factor of about 2 between the flat and hilly terrain on the one hand, and the mixed terrain on the other. Thus it appears that the most complexity in the terrain is in areas of moderate relief.

It would be expected that this fact is also evident in the bifurcation or stream branching ratio, which can be computed for any two consecutive stream levels. This ratio is the degree of diminution of stream segments by Strahler order as order increases. These ratios remain in the range from 0.0 to 0.832, with a mean of 0.413. Figure 4 shows the

results of averaging these values across stream orders for each DEM resolution, and plotting against terrain type. Hilly terrain produces the lowest branching ratios, exceeded by flat and then mixed. The mixed terrain shows little variation across resolution (with a slight drop for the SRTM), while the flat systematically increases and the hilly systematically decreases. This implies that mixed terrain is structurally similar at varying resolutions, while hilly terrain generates more low order streams and flat terrain generates more high order (or lacks low order). In fact, the flat terrain tends to be dominated in the averaging by the rapid drop from second order to third order streams, with far fewer first order streams. These data imply that while hilly terrain has lower branching ratios than flat or mixed terrain, scale-related impacts on feature extraction are limited to the network size, rather than to its topology.

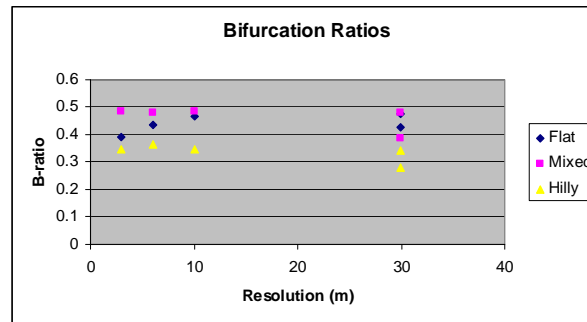


**Figure 4:** Mean Stream Bifurcation Ratios by Resolution and Strahler Level.

Next we analyzed the geometric character of the stream systems extracted from the DEMs. The raw number of streams decreases exponentially as resolution step size increases, but this effect, which we thought would be most pronounced in the hilly terrain and least in the flat, was highest at all resolutions for the mixed terrain and largely the same in form for the hilly and the flat (Figure 5). The raw number of catchments or watersheds extracted did fall into order (Figure 6), with the most catchments in the flat terrain and the lowest in the hilly. While this seems counterintuitive, the larger number of catchments at high resolution in the flat terrain is most likely due to the complexity of capturing more minor detail, and of dealing with a growing number of enclosed depressions that must be handled separately in the algorithm by filling. There was also a resolution effect. On the flat terrain the number of catchments grew as the resolution cell size became smaller, while for the mixed and hilly terrain there was less dependence on resolution.

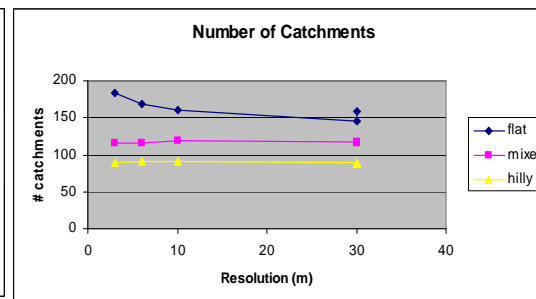
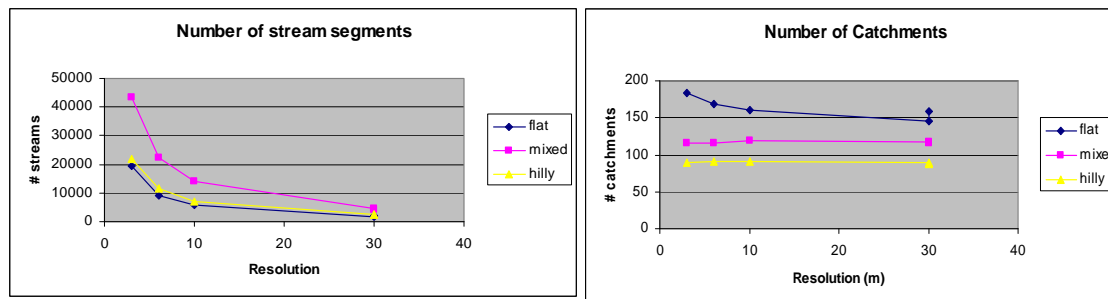


**Figure 5:** Number of Stream Segments by Terrain Type. **Figure 6:** Number of catchments by Terrain Type.

Figure 7 shows the total stream flow length, i.e. the sum of the lengths of all extracted stream segments, and figure 8 shows the mean density, i.e. the stream length divided by the number of catchments. Both show the same result, first that the mixed terrain again has the highest stream flow length and hence density, followed by hilly and far larger than flat, and second that there is little change in the value with spatial resolution, with an apparent low in the computed value at 6m, and a slight increase (except for the flat terrain) at 3m. Stream density seems somewhat robust to the resolution of the DEM, another counterintuitive result.

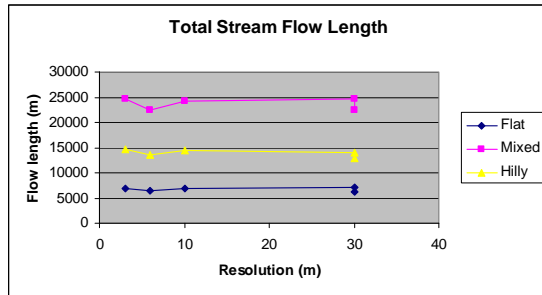


**Figure 7:** Total Stream Length by Terrain Type.

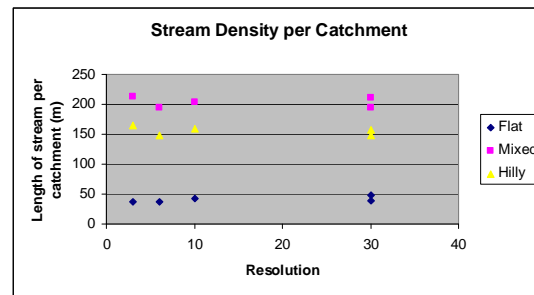


**Figure 8:** Stream Density by Terrain Type

The last cross scale comparison conducted was of the computed values for downslope flow accumulation. Feature extraction is highly sensitive to this value, it is thresholded at a low level for ridge extraction and a high level for stream delineation. The values are a grid, from which we computed the maximum (at the lowest stream outlet) and mean. These are shown in Figures 9 and 10.

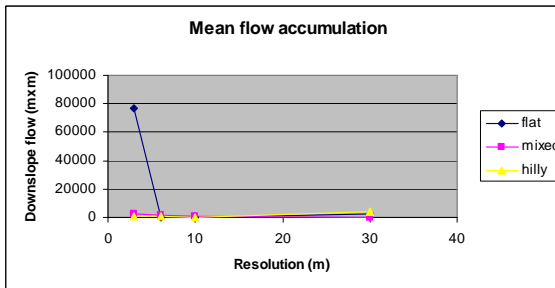
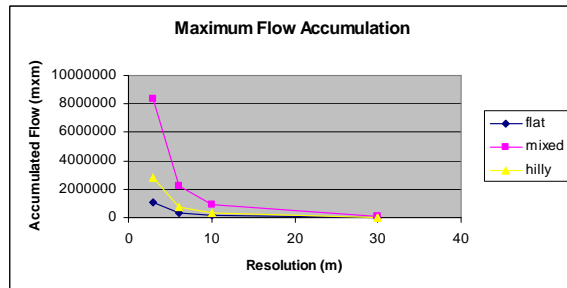


**Figure 9:** Maximum Downslope flow by Terrain Type. **Figure 10:** Mean Downslope flow by Terrain Type.

The units of the downslope flow are square meters of upstream drainage at any pixel in the grid. These values are highly resolution dependent, as is clear from Figure 9, with a simple exponential increase in upstream area at higher resolutions. This is the classic “fractal” property, when the size of a value increases as the size of the measurement scale decreases, and has been well documented for topography (Xia and Clarke, 1997). The use of the mean downslope flow reveals a major difference for the flat terrain with the 3m NED DEM. Again, we suspect that a combination of fractal surface increase and depression-filling are the cause for this phenomenon.

## CONCLUSIONS

In this study, we addressed the impact of changing spatial resolution and terrain type on the geometry of terrain surface characterized by stream delineation. Five different resolutions for each of three terrain types were analyzed to derive stream delineations for



comparison. For each set of terrain parameters, we computed: (1) the Strahler stream order and its aggregate descriptors (streams by order, and branching ratio); (2) flow path lengths and stream density; and (3) total downslope flow accumulation means and maxima. We also examined detailed focal studies to see where there were major discrepancies among the data sets.

In all, we can reexamine our initial hypotheses in the light of the findings of this research. First, we have shown that the generation of drainage and watershed features using the ArcGIS Arc Hydro tools shows major differences when tested across terrain types. Unexpectedly, the mixed terrain shows more scale-specific variance than the flat or hilly terrain, though flat terrain has some very distinct cross-scale behaviors as well. Second, as resolution in terms of cell size gets smaller, there is a measurable increase in some, but not all, terrain parameters, sufficient that there are significant resolution dependencies in the parameters. At the very least, terrain measures should be annotated by the scale at which they are measured. In some cases, the behavior may be due to the fractal property of scale self-similarity in terrain, a much-studied phenomenon. The implication is that higher resolution DEMs reveal an ever increasing amount of terrain roughness, and that perhaps the drainage feature algorithms have a “best” resolution at which they should be applied. There could also be method-produced effects of the algorithms and methodologies used in extracting the drainage, in particular. For example, the number of filled pits and the proportion of the area they occupy could impact the surface network differentially by scale. This will be the topic of further investigation.

From the LiDAR point of view, there is indeed a marked increase in the amount of variance captured in the terrain by LiDAR, and it is hypothesized that different feature extraction methods react differently to this additional variance. The 6m LiDAR data begins to show this increase in variance, but the 3m data demonstrates the increase in variance effect well. When resolutions approach the centimeter level, obviously the transformation from point cloud to DEM also comes into play. Whether this must lead to new algorithms and approaches that use LiDAR to achieve higher levels of accuracy in terrain feature extraction, a fact only suggested by these results, will also be the subject of the continuation of ongoing research.

#### **ACKNOWLEDGEMENT**

This research was supported by a grant to USCB Geography from the USGS Cooperative Ecosystem Studies Unit (CESU) of California. ICA travel for the authors was partly funded by the US National Committee, a Dangermond fellowship, and UCSB. This support is gratefully acknowledged.

#### **REFERENCES**

- BC-CARMS (2008) *LiDAR—overview of technology, applications, market features and industry*. Victoria BC: Center for Applied Sensing, Modeling and Simulation. University of Victoria.
- Carrara, P., Bordogna, G., Boschetti, M., et al. (2008) A flexible multi-source spatial data fusion system for environmental status assessment at continental scale *International Journal of Geographical Information Science*. 22, 7, 781-799.

- Chen C. C., Knoblock, C. A. and Shahabi, C. (2006) Automatically conflating road vector data with orthoimagery, *Geoinformatica*, 10, 4, 495-530.
- Chevriaux, Y. Saux, E. and Claramunt, C. (2005) A landform-based approach for the representation of terrain silhouettes. GIS05, Bremen. ACM.
- Clarke, K. C. and Lee, S-J. (2007) Spatial resolution and algorithm choice as modifiers of downslope flow computed from digital elevation models, *Cartography and Geographic Information Science*, 34, 3, 215-230.
- Deng, Y. (2007) New trends in digital terrain analysis: landform delineation, representation and classification. *Progress in Physical Geography* 31 (4), 405-419.
- Duckham, M. and Worboys, M. (2005) An algebraic approach to automated geospatial information fusion. *International Journal of geographical Information Science* 19, 5, 537-557.
- Elaksher A. F. (2008) Fusion of hyperspectral images and lidar-based dems for coastal mapping. *Optics And Lasers In Engineering*, 46, 7, 493-498
- Ling, Y., Ehlers, M., Usery, E. L., et al. (2008) Effects of spatial resolution ratio in image fusion. *International Journal of Remote Sensing*. 29, 7, 2157-2167.
- Liu, X. (2008) "Airborne LiDAR for DEM generation: some critical issues", *Progress in Physical Geography*. 32(1), pp 31-49.
- Maidment, D. R. (2002) *Arc Hydro: GIS for Water Resources*. Redlands, CA: ESRI Press.
- Kraus, K. and Pfeifer, N. (1998) "Determination of terrain models in wooded areas with airborne laser scanner data". *ISPRS Journal of Photogrammetry and Remote Sensing*. 53, 193-203.
- National Research Council (2007), *Elevation data for floodplain mapping*, National Academy Press, Washington DC.
- Nikolakopoulos, K. G. (2008) Comparison of nine fusion techniques for very high resolution data. *Photogrammetric Engineering and Remote Sensing*. 74, 5, 647-659.
- Pu, S., and Vosselman, G. (2009) Building façade reconstruction by fusing terrestrial laser points and images. *Sensors*. 9, 4525-4542.
- Rabus, B., Eineder, M., Roth, A., and Bamler, R. (2003). The shuttle radar topography mission—a new class of digital elevation models acquired by spaceborne radar. *Journal of Photogrammetry and Remote Sensing*, 57, 241–262
- Roy, D. P., Ju, J., Lewis, P. et al. (2008) Multi-temporal MODIS-Landsat data fusion for relative radiometric normalization, gap filling, and prediction of Landsat data. *Remote Sensing of Environment*. 112, 6, 3112-3130.
- Strahler, A. N. (1957), Quantitative analysis of watershed geomorphology, *Transactions of the American Geophysical Union*, 8, 6, 913–920.
- Tong, X., and Deng, S. S. (2008) Error matching detection and robust estimation adjustment approach for map conflation. *Science in China Series-E-technological Sciences*. 51, 48-61: Suppl. 1.
- Wilson, J. P. and Gallant, J. C. (2000) *Terrain Analysis*. New York: John Wiley.
- Xia, Z-G., and Clarke, K. C. (1997) Approaches to Scaling of Geo-Spatial Data in the Geosciences, Chapter 3 in Quattrochi, D. A. and Goodchild, M. (eds.) *Scale in Remote Sensing and GIS*, Boca Raton, FL: CRC Lewis, 309-360.